frontiers | Frontiers in Systems Neuroscience

TYPE Original Research
PUBLISHED 02 August 2024
DOI 10.3389/fnsys.2024.1425491

OPEN ACCESS

EDITED BY
James Joseph Chrobak,
University of Connecticut, United States

REVIEWED BY
Liming Hsu,
University of North Carolina at Chapel Hill, United States
Yikang Liu,
United Imaging Intelligence, United States

*CORRESPONDENCE
Shella Keilholz
✉ shella.keilholz@bme.gatech.edu

†These authors have contributed equally to this work

RECEIVED 29 April 2024
ACCEPTED 22 July 2024
PUBLISHED 02 August 2024

CITATION
Meyer-Baese L, Anumba N, Bolt T, Daley L, LaGrow TJ, Zhang X, Xu N, Pan W-J, Schumacher EH and Keilholz S (2024) Variation in the distribution of large-scale spatiotemporal patterns of activity across brain states.
Front. Syst. Neurosci. 18:1425491.
doi: 10.3389/fnsys.2024.1425491

Variation in the distribution of large-scale spatiotemporal patterns of activity across brain states

Lisa Meyer-Baese[1†], Nmachi Anumba[1†], T. Bolt[1], L. Daley[1], T. J. LaGrow[2], Xiaodi Zhang[1], Nan Xu[1], Wen-Ju Pan[1], E. H. Schumacher[3] and Shella Keilholz[1*]

[1]Wallace H. Coulter Department of Biomedical Engineering, Georgia Institute of Technology, Emory University, Atlanta, GA, United States, [2]Electrical and Computer Engineering, Georgia Institute of Technology, Atlanta, GA, United States, [3]Psychology, Georgia Institute of Technology, Atlanta, GA, United States

A few large-scale spatiotemporal patterns of brain activity (quasiperiodic patterns or QPPs) account for most of the spatial structure observed in resting state functional magnetic resonance imaging (rs-fMRI). The QPPs capture well-known features such as the evolution of the global signal and the alternating dominance of the default mode and task positive networks. These widespread patterns of activity have plausible ties to neuromodulatory input that mediates changes in nonlocalized processes, including arousal and attention. To determine whether QPPs exhibit variations across brain conditions, the relative magnitude and distribution of the three strongest QPPs were examined in two scenarios. First, in data from the Human Connectome Project, the relative incidence and magnitude of the QPPs was examined over the course of the scan, under the hypothesis that increasing drowsiness would shift the expression of the QPPs over time. Second, using rs-fMRI in rats obtained with a novel approach that minimizes noise, the relative incidence and magnitude of the QPPs was examined under three different anesthetic conditions expected to create distinct types of brain activity. The results indicate that both the distribution of QPPs and their magnitude changes with brain state, evidence of the sensitivity of these large-scale patterns to widespread changes linked to alterations in brain conditions.

KEYWORDS

resting state fMRI, spatiotemporal dynamic analysis, dynamic functional connectivity, brain state, functional connectivity

Introduction

Resting state functional magnetic resonance imaging (rs-fMRI) captures the spatiotemporal organization of the intrinsic activity of the brain and is a powerful translational tool for understanding normal and pathological brain function in humans and animals (Biswal et al., 1995; Greicius et al., 2004; Sorg et al., 2007; Pan et al., 2011; Zhang et al., 2020; Xu et al., 2022, 2023a). Recent work in healthy human subjects has shown that most of the features of rs-fMRI data, including functional connectivity, coactivation patterns, functional connectivity gradients, and modularity, can be explained by three repeated spatiotemporal patterns that cover the entire brain (Yousefi and Keilholz, 2021; Bolt et al., 2022). These patterns, sometimes

called quasiperiodic patterns or QPPs (Majeed et al., 2009, 2011; Yousefi et al., 2018; Abbas et al., 2019a), capture cyclical activation and deactivation of brain areas and propagation of activity as areas transition between activated and deactivated phases. In humans, the first QPP describes the spatiotemporal evolution of the global signal, which contains contributions from both neural activity and widespread noise (Wong et al., 2013; Murphy and Fox, 2017; Power et al., 2017; Billings and Keilholz, 2018; Anumba et al., 2023). QPP2 captures the alternating activation and deactivation of the default mode network (DMN) and task positive network (TPN), which has been implicated in variability in task performance (Fox et al., 2005, 2006; Thompson et al., 2013). In the third QPP, somatomotor areas and visual areas activate and deactivate with opposite phases.

The spatial structure of the intrinsic activity captured by QPPs is remarkably similar across individuals and even across species (Yousefi et al., 2018; Xu et al., 2022). While changes in functional connectivity, for example, are observed during deep sleep and anesthesia (Peltier et al., 2005; Horovitz et al., 2008, 2009), they are typically subtle. This stereotyped intrinsic activity interacts with tasks or stimuli and accounts for a portion of intraindividual variability (Fox et al., 2006; Thompson et al., 2013; Belloy et al., 2021; Xu et al., 2023a; Seeburger et al., 2024). Researchers increasingly use the term "brain state" to refer to commonly repeated configurations of brain activity. Because these states are dominated by intrinsic activity, and because intrinsic activity consists mostly of a few QPPs, we hypothesize that the relative expression of these spatiotemporal patterns defines brain states and reflects nonlocalized changes in brain activity related to phenomena such as arousal, focus, or emotion. For example, the global signal has previously been linked to arousal levels, with its amplitude increasing as arousal decreases (Wong et al., 2012, 2013; Liu and Falahpour, 2020). Given the close links between QPP1 and the global signal, and between global signal and arousal, it seems likely that QPP1 might increase as arousal decreases. Preliminary data suggest that neuromodulatory nuclei play a role in driving these patterns of activity (Abbas et al., 2018), consistent with a potential link to changing conditions in the brain.

QPP2 also has potential links to arousal and/or attention. Prior studies of spatiotemporal patterns have typically utilized global signal regression, which suppresses QPP1 and makes QPP2 the primary pattern (Abbas et al., 2019a,b; Xu et al., 2023a; Seeburger et al., 2024). QPP2 is closely related to anticorrelated activity in the DMN and TPN, which has long been linked to task performance. In both humans and rats, QPP2 interacts with incoming stimuli and influences the resulting activation (Belloy et al., 2021; Xu et al., 2023a). The spatial extent of the activity can be modulated by task performance in humans (Abbas et al., 2019a), and the magnitude of the difference between activated and deactivated brain regions is greater when subjects are 'in the zone' on a finger tapping task (Seeburger et al., 2024), but reduced in patients with ADHD compared to controls (Abbas et al., 2019b). These converging findings suggest that QPP2 also has ties to attention and/or arousal, but because QPP1 was not examined, it is difficult to compare the relative sensitivity of the two patterns. Little work to date has examined QPP3.

In this study, we aim to understand how alterations in brain state affect the first three QPPs, taking a two-pronged approach. First, we perform further analysis of the human rs-fMRI data examined in Bolt et al. (2022), to determine whether the magnitude and/or relative incidence of different QPPs is constant or variable over the course of a scan where subjects may experience fluctuating arousal levels. We then examine rs-fMRI data acquired in rodents, where brain state is manipulated using three anesthetic conditions with different mechanisms of action and different effects on neural activity and vascular tone. Results from both species suggest that the strength and relative distribution of QPPs provide information about changes in brain state.

Methods

Overview

Resting state fMRI from human subjects was obtained from the Human Connectome Project (Van Essen et al., 2013) and used in Bolt et al. (2022) to show that large-scale spatiotemporal patterns explain most of the spatial structure of functional connectivity. We built on the original analysis of this data to examine the distribution of QPPs over the course of the scan. For rodents, all experimental protocols were approved by the Institutional Animal Care and Use Committee at Emory University. We first obtained rs-fMRI data from a small group of animals during free breathing or mechanical ventilation phase-locked to MRI acquisition to evaluate respiratory noise and motion, which can both contribute to large scale patterns of activity such as the global signal (Power et al., 2017). We then examined rs-fMRI data from mechanically-ventilated rats under three anesthetic conditions (reported previously in Anumba et al., 2023) to examine the spatiotemporal organization of intrinsic brain activity under conditions of minimal noise.

Human Connectome Project data and analysis

We examined the magnitude of the time courses of the first three QPPs in the same 50 unrelated subjects (21 males) from the Human Connectome Project dataset used in the Bolt et al. paper (GE-EPI; TR 720 ms, 1,200 volumes) (Bolt et al., 2022). To briefly summarize the prior analysis, the data was in surface based format (cifti) and had been denoised using HCP's ICA-based algorithm. Spatial smoothing and bandpass filtering (0.01–0.1 Hz) were applied prior to further analysis. QPPs were extracted using the complex PCA approach described in Bolt et al. (2022) with code available at https://github.com/tsb46/complex_pca. Ten components (QPPs) were obtained and varimax rotation was performed. The explained variance for each component and the magnitude and phase of each component at each time point were obtained. Based on an elbow in the explained variance, three QPPs were retained for the remaining analysis (Bolt et al., 2022).

Complex PCA calculates a magnitude and phase for each QPP at each timepoint. To build upon the prior analysis and investigate the occurrence of different QPPs over the course of the scan, each time point was assigned a value (e.g., 1, 2, 3) that corresponded to the magnitude of the strongest QPP at that time point. This is a simplistic definition of brain state, but provides clear visualization of changes in the dominant QPP over time. Carpet plots of the state occurrence for each time point from each participant were created and sorted across time and across subject. The relative incidence of each state was

calculated for each subject, and substantial intersubject variability was observed. To further explore this variability, subjects were clustered into two groups based on the mean and standard deviation of each complex principal component over the course of the scan (6 features) using the k-means algorithm in Matlab (Euclidean distance, 50 repetitions; $k = 2$ chosen based on Silhouette criteria). The resulting groups were sorted across time. It was observed that the distribution of QPPs changed over the course of the scan, so we calculated the mean and standard deviation of the magnitude of each QPP for the first 200 and last 200 time points separately to detect any changes in QPP strength over the course of the scan. A paired *t*-test was applied for each QPP to identify significant changes.

Note that Bolt et al. used complex principal component analysis (cPCA) to extract the spatiotemporal patterns and that they are referred to as cPCs in Bolt et al. (2022). For consistency with prior work, we use the term QPP in this manuscript. The patterns extracted by the original QPP pattern-finding algorithm (Majeed et al., 2011; Yousefi et al., 2018; Yousefi and Keilholz, 2021) and the cPCA approach are highly similar (Bolt et al., 2022).

Rodent data acquisition

One of the advantages of the rodent model is that motion-related noise is minimal relative to human studies. The rats are anesthetized and head-fixed, nearly eliminating motion of the head. However, the motion of the chest during respiration can affect the magnetic field at the brain, adding respiratory noise, and this effect is particularly strong in rodents, where the field strength is high and the chest is in close proximity to the head (Kalthoff et al., 2011). To minimize effects of differences in non-neural processes such as respiration across anesthetic conditions, we implemented a protocol where the rats are paralyzed, intubated and mechanically ventilated at frequency locked to image acquisition, ensuring that each slice is acquired at the same respiratory phase for each imaging volume. As shown in the Supplementary material, this method reduces unwanted variability in rs-fMRI compared to the same rats breathing freely. The protocol was then applied in rats under three different anesthetic conditions to characterize the contributions of QPPs under each condition.

Acquisition of the data used for this analysis was reported previously (Anumba et al., 2023). Briefly, eight male Sprague Dawley rats (299 g – 339 g, Charles River) were intubated and ventilated at approximately 1 Hz. An infusion line was inserted subcutaneously to administer the paralytic pancuronium at a rate of 1.5 mg/kg/h for the duration of the scan. For the comparison of different anesthetic conditions, rats were scanned consecutively under three protocols: 1.5% isoflurane (ISO), dexmedetomidine (DMED) only, and a combination of dexmedetomidine with a low dose isoflurane (ISODMED). These anesthetics have different effects on brain activity, and so would be expected to produce different brain states. Images were acquired nearly continuously as animals moved from one anesthetic condition to another and were allowed to stabilize under each anesthetic, which took a different amount of time for each rat. Animals were first scanned for an average of 35 min under ISO. Rats were then subcutaneously injected with a 0.025 mg/kg bolus of DMED, taken off ISO 5 min later, and then switched to a 0.05 mg/kg/h subcutaneous infusion of DMED at 10 min post-bolus. The animals were then scanned again for an average of 61 min. Afterwards, the animals were introduced to a low dose of ISO at 0.5% in combination with the 0.05 mg/kg/h subcutaneous infusion of DMED. The animals were then scanned for a final time for 49 min on average. A table with the exact timing of anesthetic introduction and image acquisition for each rat is included in the supporting information of Anumba et al. (2023). For this study of changing brain states, we included data from the times when animals were transitioning from one anesthetic to another, and show all time points from all animals for full transparency.

All rodent imaging was performed on a 9.4 T/20 cm horizontal bore small animal MRI system with a homemade transmit/receive surface coil ~2 cm in diameter. Anatomical scans were obtained using a T2-weighted RARE sequence [TR = 3,500 ms, TE = 11 ms, 24 axial slices, 0.5 mm (Greicius et al., 2004) isotropic voxels]. Resting state fMRI scans were acquired using a gradient-echo echo-planar imaging (EPI) sequence with field of view (FOV) 35 mm × 35 mm, matrix size 70 × 70, and 24 axial slices for whole-brain coverage, resulting in isotropic voxels of 500 microns (TE = 15 ms, TR = 2,000 ms) with partial Fourier encoding (encoding factor 1.4) to reduce the length of the echo train. A 3-volume reversed blip EPI image with the same parameters was acquired before each longer functional scan for TOPUP correction (Andersson et al., 2003; Smith et al., 2004). EPI scans included saturation bands to minimize signal from frontal and ventral regions outside the brain and were preceded by 10 dummy scans to ensure the signal reached steady state.

All rs-fMRI scans for the mechanically-ventilated rats were phase-locked, meaning that the time between subsequent images was set to a multiple of the animal's respiratory rate so that each image was acquired during the same phase of the respiratory cycle (Anumba et al., 2023) (Figure 1). This practice was adopted here to limit any effects of motion that could arise due to movement of the chest cavity and volumes being imaged at different points in the respiratory cycle. Images were acquired at a frequency of every other breath, or 2 Hz (TR = 2,000 ms).

Preprocessing of rodent data

Preprocessing was performed using FSL (Jenkinson et al., 2012) and Analysis of Functional NeuroImages (AFNI) (Cox, 1996). Distortion correction was applied to all scans using FSL Topup and registration to the 30th volume of each scan was performed using AFNI 3dVolReg. Motion regression (6 parameters and up to 2 polynomials) and bandpass filtering (0.01–0.25 Hz) were performed in one step using AFNI 3dTProject. The bandpass range was chosen to accommodate all anesthetic conditions, as previous work has shown that BOLD is coherent with local field potentials for different frequencies under DMED (0.01–0.25 Hz) and ISO (0.01–0.1 Hz) (Pan et al., 2013). Spatial smoothing was not applied to this data. All scans were aligned to a single subject using direct, linear EPI to EPI registration via AFNI 3dAllineate and concatenated.

Extraction and comparison of QPPs in rats

Data from all three anesthetic conditions were concatenated to enforce a common definition of QPPs. As in humans, QPPs were extracted using the complex PCA approach described in Bolt et al. (2022) with code available at https://github.com/tsb46/complex_pca.

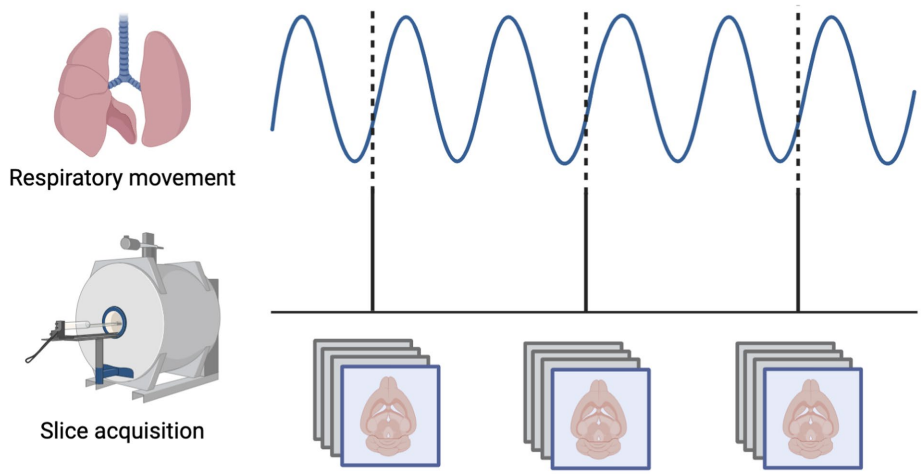

FIGURE 1
Mechanical ventilation in rats enables phase-locked acquisition of rs-fMRI data. The respiratory phase is continuously monitored and the interval between subsequent images is set so that each slice is always obtained at the same phase of the respiratory cycle, minimizing variability related to movement of the chest within the magnetic field.

Ten QPPs were obtained and varimax rotation was performed. The explained variance for each QPP and the magnitude and phase of each QPP at each time point were obtained. Based on the amount of variance explained, the top three QPPs were retained. The magnitude and phase of these QPPs were mapped, and movies that better demonstrate the evolution of activity over time were created. To investigate the occurrence of different components across scans and across rats, each time point was assigned a value (e.g., 1, 2, 3) based on the magnitude of the strongest QPP at that time point. Visual representations of the occurrence of states were created for all time points from each rat in each condition. The mean incidence of each state and the mean magnitude of each QPP for each condition were calculated. Repeated measures ANOVA was applied for each component to determine whether there was a significant effect of subject or condition.

Results

Distribution of QPPs in humans

The spatiotemporal patterns of the three QPPs can be found in Bolt et al. (2022). The relative incidence of QPPs exhibited clear variability over time in HCP data. The number of subjects exhibiting QPP1 (i.e., global signal) at each time point increases at the expense of QPP2, while the incidence of QPP3 remains relatively stable (Figure 2A). When the QPPs are sorted for each subject rather than each time point, it is apparent that some subjects have relatively high ratios of QPP1 to QPP2, and others have much lower ratios (Figure 2C). To further probe this finding, subjects were clustered into two groups with different patterns of QPP expression. For cluster 1, 41.8% of the time points were assigned to pattern 1, 22.7% to pattern 2, and 25.8% to pattern 3. For cluster 2, 23.9% of the time points were assigned to pattern 1, 21.6% to pattern 2, and 18.9% to pattern 3. When carpet plots are separated by cluster, it becomes clear that in cluster 1, QPP1 dominates and increases over the course of the scan at the expense of QPP2, while in cluster 2, time points are more evenly distributed across the three QPPs and maintain their relative representation over time (Figures 2D,E). QPP3 was more evenly distributed across clusters than QPPs 1 and 2. As a complementary analysis, the average magnitude of each QPP (rather than its relative incidence) across the first and last 200 time points of each scan was calculated across all subjects (avoiding the slow shift in distribution over the middle of each scan). The magnitude of each QPP was significantly greater ($p < 0.001$) at the end of the scan than at the beginning of the scan, with QPP1 exhibiting the greatest change (Figure 2B). These results suggest that both the relative distribution of QPPs and their magnitudes provide information about changes in brain state that occur over the course of the scan.

Spatiotemporal patterns in ventilated rats with phase-locked acquisition

QPPs were detected across all anesthetic conditions. A plot of the variance explained by each component exhibited an "elbow" around 4 QPPs (Figure 3), similar to that observed at 3 QPPs in humans (Figure 3 of Bolt et al., 2022). While the first component explains a larger percentage of the variation than the other two, the difference between the first component and the remaining components is less pronounced than in humans. Three view snapshots of the magnitude maps are shown for the first 3 QPPs in Figure 3 (movies available in the Supplementary material). For consistency with human studies, the remaining analysis is shown for the top 3 QPPs. Results for all 10 components can be found in the Supplementary material.

Prior work in rodents applied global signal regression and therefore only examined QPP2. As expected, QPP1 strongly resembles the pattern of global signal obtained from the same rats (Anumba et al., 2023), consistent with the observation that QPP1 captured the global signal in humans (Bolt et al., 2022). QPP2 and QPP3 both capture aspects of lateral-medial propagation from QPPs previously observed in rats after global signal regression (Majeed et al., 2009, 2011).

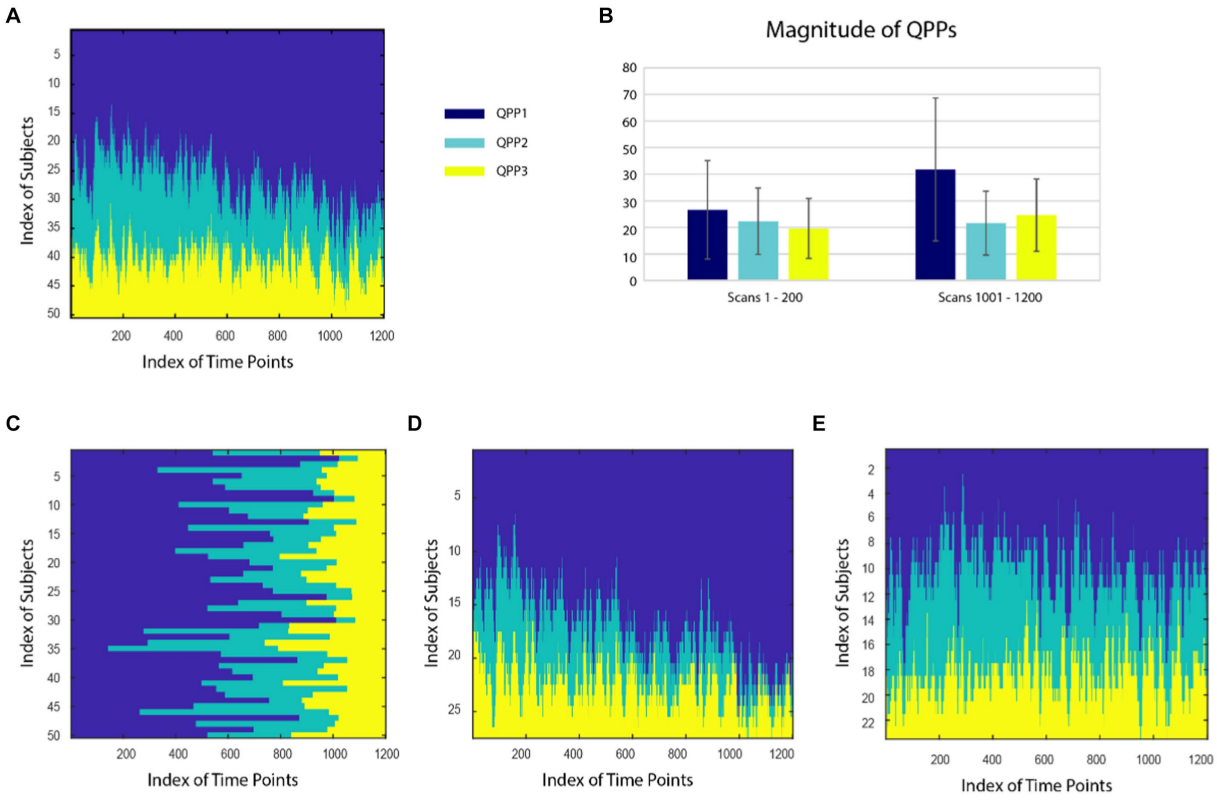

FIGURE 2
(A) Distribution of QPPs 1 (dark blue), 2 (teal), and 3 (yellow) at each timepoint for all subjects, sorted across subjects for each time point. The incidence of QPP1 increases over time and that of QPP2 decreases. **(B)** Average magnitude of each QPP in the beginning (first 200 time points) and end (last 200 time points) of the scan. The magnitude of each QPP was significantly greater ($p < 0.001$) at the end of the scan than at the beginning of the scan. **(C)** Distribution of QPPs sorted for each subject across all time points. Differences in the relative incidence of different states can be observed. When subjects are clustered into two groups, one group (27 subjects) displays an even more prominent increase in QPP1 over time **(D)**, while the distribution remains relatively constant in the second group (**E**; 23 subjects).

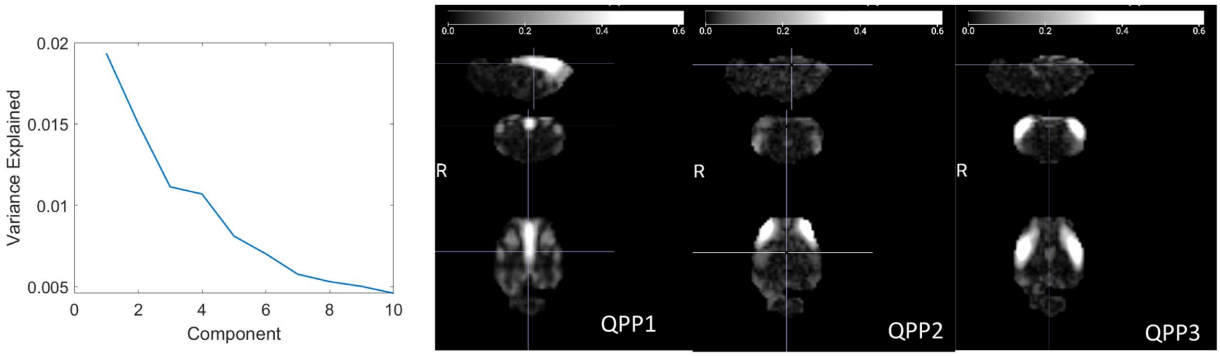

FIGURE 3
(Left) Explained variance for each QPP. An elbow occurs around 3 QPPs, similar to prior work in humans. (Right) Three directional snapshots of the whole-brain magnitude maps for the first 3 QPPs.

Distribution of spatiotemporal patterns across animals and conditions

Animals exhibited variability in the expression of the spatiotemporal patterns over the course of the scan for each anesthetic condition (Figures 4A–C). No clear difference in the expression of patterns over the course of the scan was obtained, but unlike in humans where drowsiness is common as scans progress, the rats were expected to remain in a fairly stable state for each anesthetic condition. Carpet plots were not sorted across time or animal because

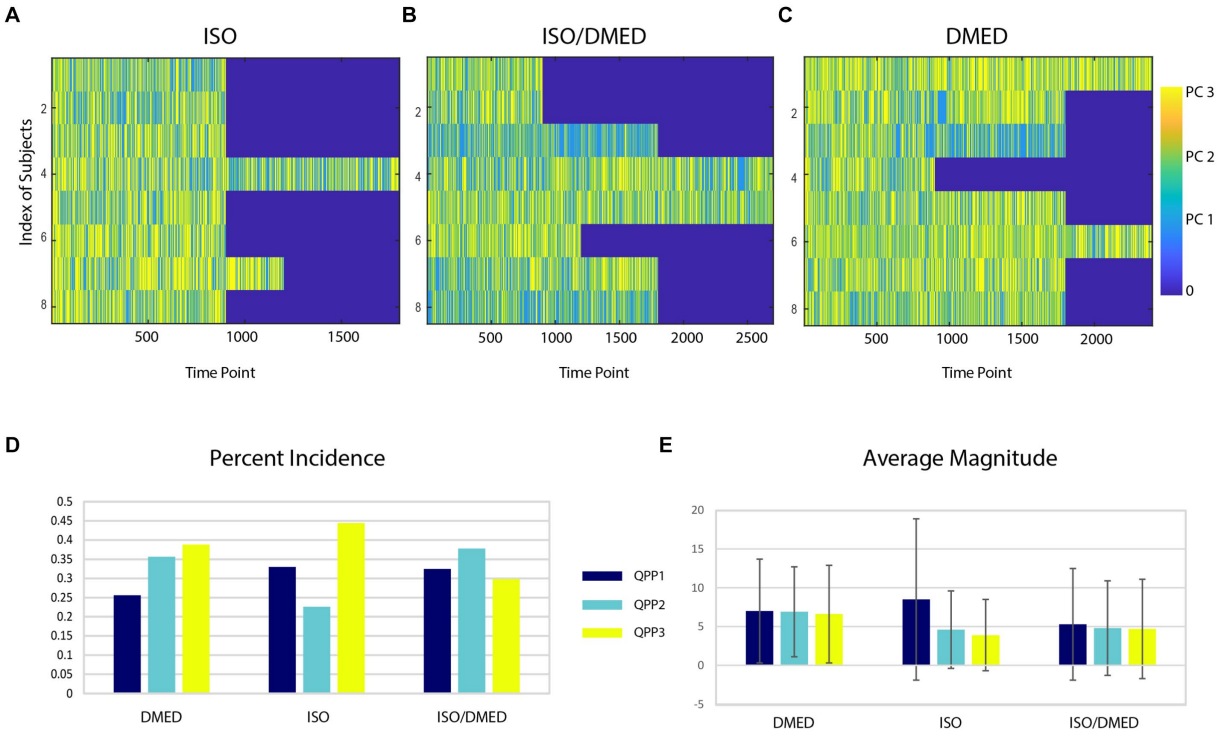

FIGURE 4
(Top) QPP state over time for each rat under different anesthetics (ISO, **A**; ISODMED, **B**; DMED, **C**). Each row contains all time points from one rat. Substantial variation can be seen across animals and within a single animal over time. **(D)** Overall percent incidence of each QPP for each of the three anesthetic conditions. Some QPPs occur more often in a single condition (e.g., 3 in ISO), or are reduced in particular anesthetic conditions (e.g., 1 for DMED). **(E)** Average magnitude of each QPP in each condition. The magnitudes for ISO are lowest and for DMED are the highest.

the data acquisition periods varied substantially. The incidence of QPP1 was highest under ISO, while QPP2 was reduced in ISO compared to the other two conditions (Figure 4D). A paired *t*-test with Bonferroni correction for multiple comparisons was applied to the incidence for each QPP under ISO compared to DMED, the most distinct conditions. A significant reduction in QPP2 was observed under ISO ($p < 0.002$). Note, however, that this statistical approach does not account for the interdependence of the three QPPs or the varying amounts of data contributed by different animals, and is included only to provide some insight to the subject-level variability of the reported group differences. To further explore the expression of different patterns under different anesthetic conditions, the average magnitude of each component was calculated (Figure 4E). The repeated measures ANOVA found no significant effect of subject or anesthetic condition for the magnitude of any QPP, although magnitudes were lowest under ISO and highest under DMED. This suggests that the relative distribution rather than the magnitude of the various QPPs is most informative about brain state under different anesthetic conditions.

Discussion

Repeated whole-brain spatiotemporal patterns of intrinsic activity persist across a wide range of conditions and interact with transient tasks or stimuli. Based on the close links between global signal (QPP1) and arousal, and between QPP2, DMN/TPN anticorrelation, and attentional performance, we hypothesized that the relative distribution of the QPPs might reflect major changes in brain state. In humans, we observed an increase in QPP1 over the course of the scan at the expense of QPP2 that was most pronounced in a subgroup of subjects and which plausibly reflects a tendency toward increasing drowsiness over the course of the scan. In rodents, alterations in the distribution of the QPPs were observed based on the use of different anesthetics. Interestingly, in both humans and rodents, the state with presumably the lowest arousal level (i.e., the end rather than the beginning of the scan; ISO rather than DMED) has increased incidence of QPP1 relative to QPP2. This is consistent with the finding that the amplitude of the global signal increases with decreasing vigilance (Wong et al., 2012, 2013; Liu and Falahpour, 2020), and that greater anticorrelation between the DMN and TPN (reflecting a stronger contribution from QPP2) is linked to better attentional performance (Thompson et al., 2013; Seeburger et al., 2024).

One of the key questions in the analysis of spatiotemporal patterns of activity is which features are most sensitive to changing conditions in the brain. The spatiotemporal patterns themselves are markedly similar across individuals and across scans (Yousefi et al., 2018). We hypothesized that changes in brain state would be related to the relative distribution of the most prominent patterns, the magnitude of the patterns, or both. Our results suggest that both magnitude and incidence can be affected by changes in brain state. In humans, both the magnitude and incidence of QPP1 increase over the course of the scan, but in rats there is little differentiation in the magnitude of the QPPs across anesthetic conditions, while the relative incidence of the

QPPs exhibits greater variability. The magnitude of QPPs has not been typically been examined in prior work, but one study has shown that the strength of the anticorrelation captured by QPP2 is weaker in subjects with ADHD compared to controls (Abbas et al., 2019b). While a different algorithm was employed in that study, those results are consistent with a lower magnitude for QPP2 in ADHD. Together, these findings support the sensitivity of both magnitude and incidence of QPPs to changes in brain state.

Source of QPPs

Despite the prominence of QPPs in rs-fMRI, little is known about the mechanisms that organize brain-wide activity into these few repeated spatiotemporal patterns. Multimodal studies have linked them to infraslow neural activity (Thompson et al., 2014; Grooms et al., 2017), and QPPs exhibit reduced magnitude when slow waves are suppressed (Khalilzad Sharghi et al., 2022), but these low frequency electrical fluctuations are themselves understudied. Structural connectivity undoubtedly plays a role in the organization of intrinsic brain activity, as shown by modeling studies that recreate much of the structure of functional connectivity by using a network representation of the brain's structural connections along with a variety of neural mass models. In particular, a study in humans reproduces the division of the brain into two large, anticorrelated networks as observed in QPP2 in humans based on the structural connections and neural mass models (Kashyap and Keilholz, 2019), although the patterns lack the complexity and propagation observed empirically. In rats, after surgical severance of the corpus callosum, QPPs continue to occur but their typical bilateral structure is disrupted (Magnuson et al., 2014), more evidence of a structural component. Nevertheless, structure alone does not readily explain the propagation along the cortex and subcortical structures that is observed in the QPPs.

One potential source for brain-wide modulation is input from one or more deep brain neuromodulatory nuclei. For example, the basal forebrain the primary source of cholinergic projections to the cortex, and prior work has shown that unilateral stimulation of the NB alters GS (QPP1) ipsilaterally (Turchi et al., 2018). Other nuclei, such as the noradrenergic locus coeruleus or the serotonergic raphe nuclei, may also play a role. These systems are deeply interconnected and well-positioned to coordinate brain-wide patterns of activity. We have shown that QPPs distinguish between healthy mice and an Alzheimer's model (Belloy et al., 2018a); are altered in humans with ADHD compared to controls (Abbas et al., 2019b); influence reaction time on a simple vigilance task (Abbas et al., 2016); are altered during task performance (Abbas et al., 2019a); and interact with sensory stimuli (Xu et al., 2023b), all of which are consistent with a role for neuromodulatory input. Further experiments with chemogenetic or optogenetic manipulation of these nuclei (Zerbi et al., 2019) may shed more light upon their role in the organization of QPPs.

Global signal

The global signal is known to contain contributions from noise as well as widespread neural activity (Liu et al., 2017). We assessed the relative levels of noise in mechanically-ventilated compared to free-breathing rats based on temporal SNR. Temporal SNR can be difficult to interpret for BOLD fluctuations because multiple factors (some wanted, some unwanted) contribute to the amplitude of the fluctuations. In this case, we interpret the increased tSNR of the global signal as reflective of a greater contribution from neural activity relative to noise. Both the higher mean framewise displacement and the widespread increase in power in the global signal for the freely-breathing rats point to a higher noise level in the data.

In the mechanically-ventilated rats where global signal was reduced, the primary spatiotemporal pattern exhibited high amplitude along the midline, consistent with the regions most correlated to the global signal in Anumba et al. (2023). While this pattern explains the largest portion of the variance observed in the BOLD signal, the proportion is relatively less than in humans. We believe the primary explanation is the lack of smoothing in the rodent data compared to standard smoothing in the human data. Another possible explanation is that the signal in the ventilated rats includes fewer contributions from noise and from respiration in particular. This is evident from the lack of correlation between the global signal and nearby non-brain tissue described in Anumba et al. (2023). Our recent work in humans links the primary spatiotemporal pattern to changes in EEG power, pupil diameter, heart rate variability, respiratory volume, skin conductance, and peripheral vascular tone (Bolt et al., 2023), suggesting that the primary component in rats may also be linked to autonomic signaling. The animals are also anesthetized, which is likely to reduce the contribution of fluctuations in arousal.

Relative occurrence across states

The three anesthetic states have all been used for rs-fMRI in rodents (Pawela et al., 2009; Pan et al., 2011; Magnuson et al., 2014; Brynildsen et al., 2017; Anumba et al., 2023), although most recently ISODMED has dominated the literature (Brynildsen et al., 2017). These anesthetics have a wide range of effects on neural activity (from enhancement of low frequency activity under DMED to cortex-wide spiking under deep ISO) and the vasculature (vasoconstriction under DMED, vasodilation under ISO). Anesthetics can also affect physiological processes such as respiration and heart rate, but respiratory effects were minimized by the combination of mechanical ventilation and phase-locked acquisition, and cardiac pulsation has relatively little effect on rs-fMRI in rats (Williams et al., 2010). Interestingly, the relative incidence of QPPs 1 and 2 were reversed from ISO to DMED, possibly reflecting the relatively deep anesthesia obtained with ISO and the lighter sedation that occurs under DMED. Our results are consistent with our expectation that these different anesthetic regimens result in quite different brain states. Note that because we included all of the data acquired as anesthetics were changed, the differences between states may even be underestimated.

Comparison to existing work in rodents

Prior studies in rodents had limited brain coverage and examined only a single QPP (Majeed et al., 2009, 2011; Pan et al., 2013; Thompson et al., 2014, 2015). In this study, we expand upon prior work to characterize multiple QPPs throughout the whole brain under three anesthetics expected to result in very different brain states.

We show that mechanical ventilation phase-locked to image acquisition reduces apparent motion even in head-fixed, anesthetized rats where motion is minimal due to the reduced variability in disruption from the motion of the chest in the magnetic field. Under these ideal conditions, three spatiotemporal patterns of BOLD fluctuations explain much of the variance in the signal, as in humans, across anesthetic conditions. QPPs have been observed in species from mice to humans (Majeed et al., 2009, 2011; Belloy et al., 2018a,b; Yousefi et al., 2018; Abbas et al., 2019a; Yousefi and Keilholz, 2021), which is not surprising given that the functional networks obtained based on the patterns of intrinsic activity are also present across species (Xu et al., 2022), although the correspondence between particular QPPs across species has yet to be examined. Thus, the clear differences in the magnitude and incidence of the patterns that demonstrate their sensitivity to induced changes in whole brain activity suggest that the relative expression of different patterns may provide information about the changes in brain state related to nonlocalized processes such as autonomic processing, arousal, emotion, and more across species.

Limitations

In the data from humans, no simultaneous measure of arousal (e.g., EEG) was available. Nevertheless, it has been shown that drowsiness tends to increase over the course of the scan (Gonzalez-Castillo et al., 2022), and our results are consistent with these findings. The assignment of each time point to a single dominant QPP (1, 2, or 3) provides a simplistic view of the current brain state. While well-suited to the current investigation of changes in brain state, a more nuanced definition based on the relative magnitudes of all QPPs might provide further insight.

In the rodents, while phase-locked acquisition reduces noises, it has drawbacks in that it requires more invasive preparation (intubation) and reduces flexibility in the choice of TR, which must be a multiple of the respiratory cycle. It may also have more subtle drawbacks related to alterations arising from the lack of top-down control, although bottom-up feedback is maintained (Tu and Zhang, 2022).

For the anesthesia study in rats, data from all conditions was concatenated. A preliminary analysis run on separate data for each condition suggested that the spatiotemporal patterns extracted were similar, supporting concatenation. The observation that all three patterns are observed in all three states also suggests that concatenation is appropriate. Further work should investigate more subtle differences in the spatiotemporal patterns and timing across groups.

Data availability statement

The raw data supporting the conclusions of this article will be made available by the authors, without undue reservation.

Ethics statement

Ethical approval was not required for the study involving humans in accordance with the local legislation and institutional requirements. Written informed consent to participate in this study was not required from the participants or the participants' legal guardians/next of kin in accordance with the national legislation and the institutional requirements.

Author contributions

LM-B: Conceptualization, Data curation, Formal analysis, Investigation, Methodology, Software, Validation, Visualization, Writing – original draft, Writing – review & editing. NA: Conceptualization, Data curation, Formal analysis, Investigation, Methodology, Software, Validation, Visualization, Writing – original draft, Writing – review & editing. TB: Methodology, Resources, Software, Writing – review & editing. LD: Methodology, Writing – review & editing. TL: Methodology, Resources, Writing – review & editing. XZ: Methodology, Resources, Writing – review & editing. NX: Methodology, Resources, Writing – review & editing. W-JP: Data curation, Investigation, Methodology, Resources, Software, Supervision, Writing – review & editing. ES: Methodology, Supervision, Writing – review & editing. SK: Conceptualization, Formal analysis, Funding acquisition, Investigation, Methodology, Project administration, Resources, Software, Supervision, Validation, Visualization, Writing – original draft, Writing – review & editing.

Funding

The author(s) declare that financial support was received for the research, authorship, and/or publication of this article. This work was supported by Emory's Center for Systems Imaging Core, NIH 1R01 MH111416, 1R01NS078095, 1R01AG062581.

Conflict of interest

The authors declare that the research was conducted in the absence of any commercial or financial relationships that could be construed as a potential conflict of interest.

Publisher's note

Supplementary material

The Supplementary material for this article can be found online at: https://www.frontiersin.org/articles/10.3389/fnsys.2024.1425491/full#supplementary-material

References

Abbas, A., Bassil, Y., and Keilholz, S. (2019b). Quasi-periodic patterns of brain activity in individuals with attention-deficit/hyperactivity disorder. *Neuroimage Clin.* 21:101653. doi: 10.1016/j.nicl.2019.101653

Abbas, A., Belloy, M., Kashyap, A., Billings, J., Nezafati, M., Schumacher, E. H. E. H., et al. (2019a). Quasi-periodic patterns contribute to functional connectivity in the brain. *NeuroImage* 191, 193–204. doi: 10.1016/j.neuroimage.2019.01.076

Abbas, A., Majeed, W., Thompson, G., and Keilholz, S. D. Phase of quasi-periodic patterns in the brain predicts performance on psychomotor vigilance task in humans. *Proc. Int. Soc. Magn. Reson. Med.* (2016):1192.

Abbas, A., Nezafati, M., Thomas, I., and Keilholz, S. D. (2018). Quasiperiodic patterns in BOLDfMRI reflect neuromodulatory input. *Proc. Int. Soc. Magn. Reson. Med.* 8422.

Andersson, J. L. R., Skare, S., and Ashburner, J. (2003). How to correct susceptibility distortions in spin-echo echo-planar images: application to diffusion tensor imaging. *NeuroImage* 20, 870–888. doi: 10.1016/S1053-8119(03)00336-7

Anumba, N., Maltbie, E., Pan, W.-J., LaGrow, T. J., Xu, N., and Keilholz, S. (2023). Spatial and spectral components of the BOLD global signal in rat resting-state functional MRI. *Magn. Reson. Med.* 90, 2486–2499. doi: 10.1002/mrm.29824

Belloy, M. E., Billings, J., Abbas, A., Kashyap, A., Pan, W.-J., Hinz, R., et al. (2021). Resting brain fluctuations are intrinsically coupled to visual response dynamics. *Cereb. Cortex* 31, 1511–1522. doi: 10.1093/cercor/bhaa305

Belloy, M. E., Naeyaert, M., Abbas, A., Shah, D., Vanreusel, V., van Audekerke, J., et al. (2018b). Dynamic resting state fMRI analysis in mice reveals a set of quasi-periodic patterns and illustrates their relationship with the global signal. *NeuroImage*. 180. Available at: https://www.sciencedirect.com/science/article/pii/S1053811918300752

Belloy, M. E., Shah, D., Abbas, A., Kashyap, A., Roßner, S., Van Der Linden, A., et al. (2018a). Quasi-periodic patterns of neural activity improve classification of Alzheimer's disease in mice. *Sci. Rep.* 8:10024. doi: 10.1038/s41598-018-28237-9

Billings, J. C. W., and Keilholz, S. D. (2018). The Not-So-Global Blood Oxygen Level-Dependent Signal. *Brain Connect.* 8, 121–128. doi: 10.1089/brain.2017.0517

Biswal, B., Yetkin, F. Z., Haughton, V. M., and Hyde, J. S. (1995). Functional connectivity in the motor cortex of resting human brain using echo-planar MRI. *Magn. Reson. Med.* 34, 537–541. doi: 10.1002/mrm.1910340409

Bolt, T., Nomi, J. S., Bzdok, D., Salas, J. A., Chang, C., Thomas Yeo, B. T., et al. (2022). A parsimonious description of global functional brain organization in three spatiotemporal patterns. *Nat. Neurosci.* 25, 1093–1103. doi: 10.1038/s41593-022-01118-1

Bolt, T., Wang, S., Nomi, J. S., Setton, R., Gold, B. P., deB Frederick, B., et al. (2023). A unified physiological process links global patterns of functional MRI, respiratory activity, and autonomic signaling. *bioRxiv*. doi: 10.1101/2023.01.19.524818

Brynildsen, J. K., Hsu, L. M., Ross, T. J., Stein, E. A., Yang, Y., and Lu, H. (2017). Physiological characterization of a robust survival rodent fMRI method. *Magn. Reson. Imaging* 35, 54–60. doi: 10.1016/j.mri.2016.08.010

Cox, R. W. (1996). AFNI: software for analysis and visualization of functional magnetic resonance neuroimages. *Comput. Biomed. Res.* 29, 162–173. doi: 10.1006/cbmr.1996.0014

Fox, M. D. D., Snyder, A. Z. Z., Vincent, J. L. L., Corbetta, M., Van Essen, D. C. C., and Raichle, M. E. E. (2005). The human brain is intrinsically organized into dynamic, anticorrelated functional networks. *Proc. Natl. Acad. Sci. USA* 102, 9673–9678. doi: 10.1073/pnas.0504136102

Fox, M. D., Snyder, A. Z., Zacks, J. M., and Raichle, M. E. (2006). Coherent spontaneous activity accounts for trial-to-trial variability in human evoked brain responses. *Nat. Neurosci.* 9, 23–25. doi: 10.1038/nn1616

Gonzalez-Castillo, J., Fernandez, I. S., Handwerker, D. A., and Bandettini, P. A. (2022). Ultra-slow fMRI fluctuations in the fourth ventricle as a marker of drowsiness. *NeuroImage* 259:119424. doi: 10.1016/j.neuroimage.2022.119424

Greicius, M. D., Srivastava, G., Reiss, A. L., and Menon, V. (2004). Default-mode network activity distinguishes Alzheimer's disease from healthy aging: evidence from functional MRI. *Proc. Natl. Acad. Sci. USA* 101, 4637–4642. doi: 10.1073/pnas.0308627101

Grooms, J. K., Thompson, G. J., Pan, W.-J., Billings, J., Schumacher, E. H., Epstein, C. M., et al. (2017). Infraslow electroencephalographic and dynamic resting state network activity. *Brain Connect.* 7, 265–280. doi: 10.1089/brain.2017.0492

Horovitz, S. G., Braun, A. R., Carr, W. S., Picchioni, D., Balkin, T. J., Fukunaga, M., et al. (2009). Decoupling of the brain's default mode network during deep sleep. *Proc. Natl. Acad. Sci. USA* 106, 11376–11381. doi: 10.1073/pnas.0901435106

Horovitz, S. G., Fukunaga, M., de Zwart, J. A., van Gelderen, P., Fulton, S. C., Balkin, T. J., et al. (2008). Low frequency BOLD fluctuations during resting wakefulness and light sleep: a simultaneous EEG-fMRI study. *Hum. Brain Mapp.* 29, 671–682. doi: 10.1002/hbm.20428

Jenkinson, M., Beckmann, C. F., Behrens, T. E. J., Woolrich, M. W., and Smith, S. M. (2012). FSL. *NeuroImage* 62, 782–790. doi: 10.1016/j.neuroimage.2011.09.015

Kalthoff, D., Seehafer, J. U., Po, C., Wiedermann, D., and Hoehn, M. (2011). Functional connectivity in the rat at 11.7T: impact of physiological noise in resting state fMRI. *NeuroImage* 54, 2828–2839. doi: 10.1016/j.neuroimage.2010.10.053

Kashyap, A., and Keilholz, S. (2019). Dynamic properties of simulated brain network models and empirical resting-state data. *Netw. Neurosci.* 3, 405–426. doi: 10.1162/netn_a_00070

Khalilzad Sharghi, V., Maltbie, E. A., Pan, W.-J., Keilholz, S. D., and Gopinath, K. S. (2022). Selective blockade of rat brain T-type calcium channels provides insights on neurophysiological basis of arousal dependent resting state functional magnetic resonance imaging signals. *Front. Neurosci.* 16:1312. doi: 10.3389/FNINS.2022.909999

Liu, T. T., and Falahpour, M. (2020). Vigilance effects in resting-state fMRI. *Front. Neurosci.* 14:321. doi: 10.3389/fnins.2020.00321

Liu, T. T., Nalci, A., and Falahpour, M. (2017). The global signal in fMRI: nuisance or information? *NeuroImage* 150, 213–229. doi: 10.1016/j.neuroimage.2017.02.036

Magnuson, M. E. M. E., Thompson, G. J. G. J., Pan, W.-J. W.-J., and Keilholz, S. D. S. D. (2014). Effects of severing the corpus callosum on electrical and BOLD functional connectivity and spontaneous dynamic activity in the rat brain. *Brain Connect.* 4, 131011122122002–131011122122029. doi: 10.1089/brain.2013.0167

Magnuson, M. E., Thompson, G. J., Pan, W. J., and Keilholz, S. D. (2014). Time-dependent effects of isoflurane and dexmedetomidine on functional connectivity, spectral characteristics, and spatial distribution of spontaneous BOLD fluctuations. *NMR Biomed.* 27, 291–303. doi: 10.1002/nbm.3062

Majeed, W., Magnuson, M., Hasenkamp, W., Schwarb, H., Schumacher, E. H. E. H. H., Barsalou, L., et al. (2011). Spatiotemporal dynamics of low frequency BOLD fluctuations in rats and humans. *NeuroImage* 54, 1140–1150. doi: 10.1016/j.neuroimage.2010.08.030

Majeed, W., Magnuson, M., Keilholz, S. D. S. D., Majeed, M., and Keilholz, S. W. M. (2009). Spatiotemporal dynamics of low frequency fluctuations in BOLD fMRI of the rat. *J. Magn. Reson. Imaging* 30, 384–393. doi: 10.1002/jmri.21848

Murphy, K., and Fox, M. D. (2017). Towards a consensus regarding global signal regression for resting state functional connectivity MRI. *NeuroImage* 154, 169–173. doi: 10.1016/j.neuroimage.2016.11.052

Pan, W.-J., Thompson, G. J., Magnuson, M. E., Jaeger, D., and Keilholz, S. (2013). Infraslow LFP correlates to resting-state fMRI BOLD signals. *NeuroImage* 74, 288–297. doi: 10.1016/j.neuroimage.2013.02.035

Pan, W.-J., Thompson, G., Magnuson, M., Majeed, W., Jaeger, D., and Keilholz, S. (2011). Broadband local field potentials correlate with spontaneous fluctuations in functional magnetic resonance imaging signals in the rat somatosensory cortex under isoflurane anesthesia. *Brain Connect.* 1, 119–131. doi: 10.1089/brain.2011.0014

Pawela, C. P., Biswal, B. B., Hudetz, A. G., Schulte, M. L., Li, R., Jones, S. R., et al. (2009). A protocol for use of medetomidine anesthesia in rats for extended studies using task-induced BOLD contrast and resting-state functional connectivity. *NeuroImage* 46, 1137–1147. doi: 10.1016/j.neuroimage.2009.03.004

Peltier, S. J., Kerssens, C., Hamann, S. B., Sebel, P. S., Byas-Smith, M., and Hu, X. (2005). Functional connectivity changes with concentration of sevoflurane anesthesia. *Neuroreport* 16, 285–288. doi: 10.1097/00001756-200502280-00017

Power, J. D., Plitt, M., Laumann, T. O., and Martin, A. (2017). Sources and implications of whole-brain fMRI signals in humans. *NeuroImage* 146, 609–625. doi: 10.1016/j.neuroimage.2016.09.038

Seeburger, D. T., Xu, N., Ma, M., Larson, S., Godwin, C., Keilholz, S. D., et al. (2024). Time-varying functional connectivity predicts fluctuations in sustained attention in a serial tapping task. *Cogn. Affect. Behav. Neurosci.* 24, 111–125. doi: 10.3758/s13415-024-01156-1

Smith, S. M., Jenkinson, M., Woolrich, M. W., Beckmann, C. F., Behrens, T. E. J., Johansen-Berg, H., et al. (2004). Advances in functional and structural MR image analysis and implementation as FSL. *NeuroImage* 23, S208–S219. doi: 10.1016/j.neuroimage.2004.07.051

Sorg, C., Riedl, V., Muhlau, M., Calhoun, V. D., Eichele, T., Laer, L., et al. (2007). Selective changes of resting-state networks in individuals at risk for Alzheimer's disease. *Proc. Natl. Acad. Sci. USA* 104, 18760–18765. doi: 10.1073/pnas.0708803104

Thompson, G. J. G. J., Magnuson, M. E. M. E., Merritt, M. D. M. D., Schwarb, H., Pan, W.-J. W. J., Mckinley, A., et al. (2013). Short-time windows of correlation between large-scale functional brain networks predict vigilance intraindividually and interindividually. *Hum. Brain Mapp.* 34, 3280–3298. doi: 10.1002/hbm.22140

Thompson, G. J. G. J., Pan, W.-J. W.-J., and Keilholz, S. D. S. D. (2015). Different dynamic resting state fMRI patterns are linked to different frequencies of neural activity. *J. Neurophysiol.* 114, 114–124. doi: 10.1152/jn.00235.2015

Thompson, G. J. G. J., Pan, W.-J. W. J., Magnuson, M. E. M. E., Jaeger, D., and Keilholz, S. D. S. D. (2014). Quasi-periodic patterns (QPP): large-scale dynamics in resting state fMRI that correlate with local infraslow electrical activity. *NeuroImage* 84, 1018–1031. doi: 10.1016/j.neuroimage.2013.09.029

Tu, W., and Zhang, N. (2022). Neural underpinning of a respiration-associated resting-state fMRI network. *eLife* 11:e81555. doi: 10.7554/eLife.81555

Turchi, J., Chang, C., Ye, F. Q., Russ, B. E., Yu, D. K., Cortes, C. R., et al. (2018). The basal forebrain regulates global resting-state fMRI fluctuations. *Neuron* 97, 940–952.e4. doi: 10.1016/j.neuron.2018.01.032

Van Essen, D. C., Smith, S. M., Barch, D. M., Behrens, T. E. J., Yacoub, E., and Ugurbil, K. (2013). The WU-Minn human connectome project: an overview. *NeuroImage* 80, 62–79. doi: 10.1016/j.neuroimage.2013.05.041

Williams, K. A. K. A., Magnuson, M., Majeed, W., LaConte, S. M. S. M., Peltier, S. J. S. J., Hu, X., et al. (2010). Comparison of α-chloralose, medetomidine and isoflurane anesthesia for functional connectivity mapping in the rat. *Magn. Reson. Imaging* 28, 995–1003. doi: 10.1016/j.mri.2010.03.007

Wong, C. W., Olafsson, V., Tal, O., and Liu, T. T. (2012). Anti-correlated networks, global signal regression, and the effects of caffeine in resting-state functional MRI. *NeuroImage* 63, 356–364. doi: 10.1016/j.neuroimage.2012.06.035

Wong, C. W., Olafsson, V., Tal, O., and Liu, T. T. (2013). The amplitude of the resting-state fMRI global signal is related to EEG vigilance measures. *NeuroImage* 83, 983–990. doi: 10.1016/j.neuroimage.2013.07.057

Xu, N., LaGrow, T. J., Anumba, N., Lee, A., Zhang, X., Yousefi, B., et al. (2022). Functional connectivity of the brain across rodents and humans. *Front. Neurosci.* 16:816331. doi: 10.3389/fnins.2022.816331

Xu, N., Smith, D. M., Jeno, G., Seeburger, D. T., Schumacher, E. H., and Keilholz, S. D. (2023a). The interaction between random and systematic visual stimulation and infraslow quasiperiodic spatiotemporal patterns of whole brain activity. *Imaging Neurosci. (Camb.)* 1, 1–19. doi: 10.1162/imag_a_00002

Xu, N., Smith, D. M., Jeno, G., Seeburger, D. T., Schumacher, E. H., and Keilholz, S. D. (2023b). The interaction between random and systematic visual stimulation and infraslow quasiperiodic spatiotemporal patterns of whole brain activity. *NeuroImage* 276:120165. doi: 10.1016/j.neuroimage.2023.120165

Yousefi, B., and Keilholz, S. (2021). Propagating patterns of intrinsic activity along macroscale gradients coordinate functional connections across the whole brain. *NeuroImage* 231:117827. doi: 10.1016/j.neuroimage.2021.117827

Yousefi, B., Shin, J., Schumacher, E. H., and Keilholz, S. D. (2018). Quasi-periodic patterns of intrinsic brain activity in individuals and their relationship to global signal. *NeuroImage* 167, 297–308. doi: 10.1016/j.neuroimage.2017.11.043

Zerbi, V., Floriou-Servou, A., Markicevic, M., Vermeiren, Y., Sturman, O., Privitera, M., et al. (2019). Rapid reconfiguration of the functional connectome after Chemogenetic locus Coeruleus activation. *Neuron* 103, 702–718.e5. doi: 10.1016/j.neuron.2019.05.034

Zhang, X., Pan, W. J., and Keilholz, S. D. (2020). The relationship between BOLD and neural activity arises from temporally sparse events. *NeuroImage* 207:116390. doi: 10.1016/j.neuroimage.2019.116390